Warming and Freshening in the Abyssal Southeastern Indian Ocean*

GREGORY C. JOHNSON

NOAA/Pacific Marine Environmental Laboratory, Seattle, Washington

SARAH G. PURKEY

Joint Institute for the Study of the Atmosphere and Ocean, University of Washington, and NOAA/Pacific Marine Environmental Laboratory, Seattle, Washington

JOHN L. BULLISTER

NOAA/Pacific Marine Environmental Laboratory, Seattle, Washington

ABSTRACT

Warming and freshening of abyssal waters in the eastern Indian Ocean between 1994/95 and 2007 are quantified using data from two closely sampled high-quality occupations of a hydrographic section extending from Antarctica northward to the equator. These changes are limited to abyssal waters in the Princess Elizabeth Trough and the Australian–Antarctic Basin, with little abyssal change evident north of the Southeast Indian Ridge. As in previous studies, significant cooling and freshening is observed in the bottom potential temperature–salinity relations in these two southern basins. In addition, analysis on pressure surfaces shows abyssal warming of about 0.05°C and freshening of about 0.01 Practical Salinity Scale 1978 (PSS-78) in the Princess Elizabeth Trough, and warming of 0.1°C with freshening of about 0.005 in the abyssal Australian–Antarctic Basin. These 12-yr differences are statistically significant from zero at 95% confidence intervals over the bottom few to several hundred decibars of the water column in both deep basins. Both warming and freshening reduce the density of seawater, contributing to the vertical expansion of the water column. The changes below 3000 dbar in these basins suggest local contributions approaching 1 and 4 cm of sea level rise, respectively. Transient tracer data from the 2007 occupation qualitatively suggest that the abyssal waters in the two southern basins exhibiting changes have significant components that have been exposed to the ocean surface within the last few decades, whereas north of the Southeast Indian Ridge, where changes are not found, the component of abyssal waters that have undergone such ventilation is much reduced.

1. Introduction

A large amount of scientific evidence exists showing that the earth is currently warming and out of radiative equilibrium (Solomon et al. 2007). Both climate modeling (Hansen et al. 2005) and data analyses (Levitus et al. 2005) suggest that the oceans are absorbing a sub-stantial amount of heat. Quantifying ocean heat uptake is important in estimates of how much warming the earth will experience in the decades and centuries to come, and at what rate that warming will occur (Hansen et al. 2005). The deepest global analysis of ocean heat content variations of which we are aware extends to 3000 m, but only at 5-yr resolution because of data sparseness, from 1957 to 1996 (Levitus et al. 2005). Most validations of climate models using variations in ocean temperature data have been limited to the upper 750 m (Barnett et al. 2005), where data are somewhat less sparse, but there are some analyses of deeper model heat content variations as well (Gent et al. 2006).

During the 1990s the World Ocean Circulation Experiment (WOCE) Hydrographic Program (WHP)

completed a global survey of all of the major ocean basins with full-depth, high-quality, coast-to-coast hydrographic sections that were closely sampled in the vertical and the horizontal. Since then, some of these sections have been similarly reoccupied by various international research teams to study decadal variability in ocean water properties and circulation. These repeat sections allow some of the few opportunities to study abyssal ocean heat and freshwater variability on a global scale.

Here abyssal water property variations are studied in the eastern Indian Ocean by comparing data from a meridional cross section of the Indian Ocean (WHP designators I09N, I08S, and SR03) originally sampled in 1994 and 1995 during WOCE to data from the 2007 U.S. Repeat Hydrography Program (information online at http://ushydro.ucsd.edu/) reoccupation in support of the Climate Variability (CLIVAR) and Carbon Cycle Science Programs. A comparison of the data from these two occupations taken over a roughly 12-yr interval reveals significant warming and freshening in Antarctic Bottom Water (AABW; $\theta < 0°C$) in the Princess Elizabeth Trough and the Australian–Antarctic Basin of the Indian Ocean, with little abyssal change evident in the deep basins sampled to the north of the Southeast Indian Ridge.

AABWs formed off Adélie Land and in the Ross Sea are likely the primary sources of the densest, coldest abyssal waters found in the Australian–Antarctic Basin (Mantyla and Reid 1995). The Ross Sea and Adélie Land varieties of AABW flow westward along Antarctica (Bindoff et al. 2000), with a branch turning to flow northwestward, banked against the northeastern flank of the Kerguelen Plateau (Speer and Forbes 1994; Donohue et al. 1999). However, the Princess Elizabeth Trough provides a passage between the Australian–Antarctic Basin and the Weddell Sea, where even colder, denser AABW is formed. Varieties of AABW flow in both directions through the trough (Heywood et al. 1999). After entering the Australian–Antarctic Basin through the Princess Elizabeth Trough, the Weddell Sea variety of AABW also turns and flows northwestward along the northeastern flank of the Kerguelen Plateau. The Weddell Sea variety of AABW, having significantly mixed with overlying Circumpolar Deep Water (CDW) at this point, itself overlies the AABW varieties formed near Adélie Land and in the Ross Sea (which are denser in this location than the variety originating from the Weddell Sea). Before reaching the northwestern end of the Kerguelen Plateau, the bottom waters are turned eastward by the Southeast Indian Ridge and the overlying Antarctic Circumpolar Cur-

rent. Some of the AABW flows northward through the Australian–Antarctic discordance in the ridge, whereupon it spreads to fill the more northern deep basins of the eastern Indian Ocean (e.g., Donohue et al. 1999, their Fig. 1).

Changes in AABW have been noted previously in the southern reaches of the Indian Ocean, specifically the Australian–Antarctic Basin. A comparison of the abyssal potential temperature–salinity (θ–S) relations of 1936–93 data to 1994–96 data distributed throughout the Australian–Antarctic Basin suggests cooling and freshening of AABW on dense isopycnals in much of the basin, but warming of bottom temperatures (Whitworth 2002). An analysis of available data in terms of near-bottom θ–S relations off the Antarctic coast between 140° and 150°E and the 1900- and 3000-m isobaths suggests cooling and freshening between 1950 and 2001, with a slight reduction in bottom density (Jacobs 2004). Analysis of hydrographic data along 140°E (WHP designator SR03) from 1969 to 1971, 1994 to 1996, and 2002 to 2003 reveals a pattern of cooling and freshening with time on dense isopycnals in the AABW between 65° and 60°S (Aoki et al. 2005) over that time period. Analysis of θ–S relations using data at various locations in the Australian–Antarctic Basin from 1970 to 1972, from 1994 to 1995, and in 2005 again reveals cooling and freshening on the densest AABW isopycnals (Rintoul 2007).

Here, regional abyssal variability is explored using data from the 1994 and 2007 occupations of the WHP I08S and I09N sections crossing the Princess Elizabeth Trough, Australian–Antarctic Basin, South Australian Basin, and Wharton Basin. The data and their processing are described in section 2. In section 3, cooling and freshening are described in the densest portions of the θ–S relations in the Princess Elizabeth Trough and Australian–Antarctic Basin over this time period using analysis in isopycnal coordinates (on density surfaces), similar to results of the studies reviewed above. In section 4, analysis in isobaric coordinates (on pressure surfaces) is added to reveal warming and freshening significantly different from zero at 95% confidence intervals in both of these regions below about 3000 dbar, and the contribution of these changes to local sea level is estimated. In section 5, an attempt is made to put these deep changes into the context of heat and freshwater fluxes. In section 6, transient tracer data are presented to help to explore why no significant changes are observed in abyssal properties north of the Southeast Indian Ridge between the 1994 and 2007 occupations of I08S/I09N. The paper ends with a discussion of the results in section 7.
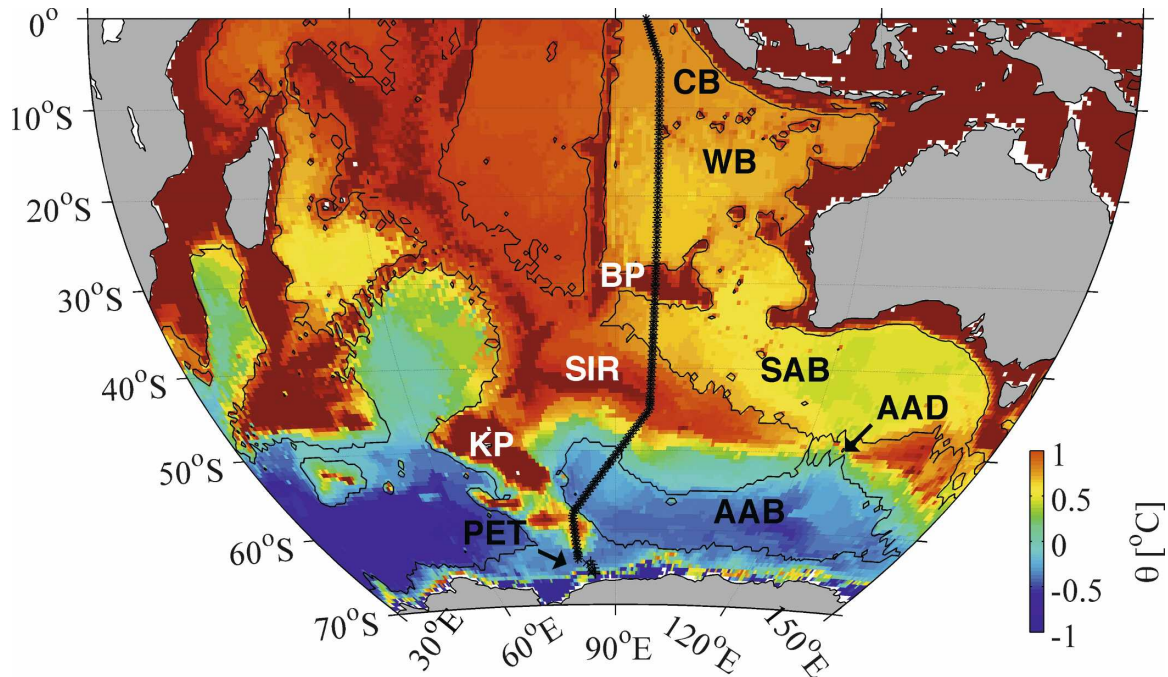
FIG. 1. Station locations used from sections with WHP designators SR03, I08S (south of about 30°S), and I09N (north of about 30°S). Stations from the 1994/95 WOCE survey (pluses) and from the 2007 U.S. Repeat Hydrography Program survey (Xs) essentially overlie each other, except for a slight divergence south of 64°S. The 4000-m isobath (thin black line) is plotted over bottom potential temperature (colors) from the WOCE Global Hydrographic Climatology (Gouretski and Koltermann 2004). Land is shaded gray. Place names indicated with abbreviations include the following: Princess Elizabeth Trough (PET; arrow), Australian–Antarctic Basin (AAB), Australian–Antarctic discordance (AAD; arrow), Kerguelen Plateau (KP; white), Southeast Indian Ridge (SIR0; white), Broken Plateau (BP; white), Wharton Basin (WB), and Cocos Basin (CB).

2. Data and processing

The data considered here form a continuous nominally meridional section stretching from Antarctica northward to the equator in the eastern Indian Ocean (Fig. 1). The section runs northward from the Antarctic continental shelf along 82°E, crossing the Princess Elizabeth Trough and the Kerguelen Plateau. At the northeastern flank of the plateau at 58.24°S it turns northeastward, crossing the Australian–Antarctic Basin. Near the crest of the Southeast Indian Ridge, at 45°S, 95°E, the section turns northward again into the South Australian Basin, crossing over the Broken Plateau near 30°S and continuing northward in the Wharton Basin. At 5°S the section turns slightly west of north to sample the deepest portion of the Cocos Basin. The section continues into the Northern Hemisphere, but only the data collected in the Southern Hemisphere are used in this analysis. Here the section is divided for analysis into the one trough and three deep basins that are crossed, hereafter referred to as the Princess Elizabeth Trough (66°–60°S), the Australian–Antarctic Basin (60°–45°S), the South Australian Basin (45°–30°S), and the Wharton Basin (30°S to the equator).

The first realization of the section analyzed here is comprised of data from three cruises taken during WOCE. WHP section I08S was sampled from 64.15° (the ice edge) to 30.30°S in December 1994 (Donohue et al. 1999). WHP section I09N was sampled from 31.3°S to its northern terminus in the Bay of Bengal in January–February 1995 (Gordon et al. 1997). The southern end of the I08S section from 64.63°S to the Antarctic continental shelf is completed using seven stations from the January 1994 occupation of WHP section SR03 (Rintoul 2007). The second realization of the section is from roughly 12 yr after the first. WHP section I08S was reoccupied from near the Antarctic continental shelf to 28.32°S in February–March 2007, and I09N is occupied from that latitude to its northern terminus in the Bay of Bengal in March–April 2007 by the U.S. Repeat Hydrography Program (online at http://ushydro.ucsd.edu/). At each station, data were collected from the surface to a depth of 10–20 m above the bottom. Station spacing was generally less than 40 n mi for both realizations of the section.

High-quality conductivity–temperature–depth (CTD) instrument data were collected on all of these cruises. [The last word of the instrument name is a misnomer,

because CTDs actually measure pressure (P), not depth.] All analyses here are performed using 1968 International Practical Temperature Scale (IPTS-68) for temperature (T), because the equation of state EOS-80 has not yet been reformulated for International Temperature Scale 1990 (ITS-90). In addition, all of the CTD salinity (S) data were calibrated to bottle samples standardized with International Association for the Physical Sciences of the Oceans (IAPSO) Standard Seawater using the 1978 Practical Salinity Scale (PSS-78). For this analysis, adjustments are made to salinity from each cruise to account for small (<0.002) offsets between different IAPSO batches used on different cruises (Kawano et al. 2006a; T. Kawano 2007, personal communication). These data are then used to derive potential temperature (θ) and potential density referenced to 4000 dbar (σ_4). These variables, along with dissolved oxygen concentrations (O_2) from water sample analyses, are used to quantify changes in water properties. Apparent oxygen utilization (AOU) values are also calculated by subtracting measured O_2 values from oxygen saturation values calculated from the salinity and potential temperature of the sample (Benson and Krauss 1984) at every location. Oxygen saturation is a strong function of temperature. The use of AOU helps to isolate O_2 changes resulting from changes in ventilation processes by removing the O_2 solubility dependence on water temperature.

Almost all of the data are believed to be accurate to at least 0.002°C for temperature and 0.003 PSS-78 for salinity. The oxygen data considered here are believed to be accurate to the WHP target of <1%. The exceptions to these accuracies are of data taken from the SR03 repeat. Because of instrument problems, these data may only be accurate to 0.02°C for temperatures below 0°C and 0.005 PSS-78 for salinity (Rosenberg et al. 1995). While these latter accuracies are less than optimal, they are smaller in magnitude than most of the signals presented here.

Analyses are carried out in isopycnal (σ_4) and isobaric (P) coordinates. After the derived fields are computed using the adjusted 2-dbar T, S, and P data from the CTD stations, they are low-passed vertically with a 40-dbar half-width Hanning filter. The results are then interpolated to a 10-dbar pressure grid for analysis. In addition, fields for $P > 1000$ dbar are also interpolated to a finely spaced σ_4 grid. The vertically gridded datasets are then interpolated onto an evenly spaced latitudinal grid at 2′ spacing using a space-preserving piecewise cubic Hermite interpolant at each pressure (and σ_4) level. This spacing matches that of a high-resolution bathymetric dataset used here generated by merging satellite altimetry data with bathymetric

soundings (Smith and Sandwell 1997). The bathymetry from this dataset along each section is used as a mask to eliminate data that have been interpolated to locations below the ocean.

The two section realizations generally are very close to each other in longitude. However, their longitudes diverge slightly south of 64°S where ice conditions impose constraints on sampling. Because the isobaths in between the sections in this latitude range generally run nearly east–west, the longitudes for these stations are simply considered to be the average between the lines for the purposes of this analysis. However, because the section longitudes do diverge slightly below 64°S, the maximum sampled pressures rather than the satellite bathymetry are linearly interpolated to the latitudinal grid for bathymetric masking in this region. In addition, the two sections diverge in longitude north of the equator, which is why the analysis here is limited to the Southern Hemisphere.

3. Isopycnal water property variations

Examination of mean θ–S relations (Fig. 2) estimated on the isopycnal grid for the Princess Elizabeth Trough and the Australian–Antarctic Basin reveals significant changes between 1994/95 and 2007 for $\theta < 0.0°C$ ($\sigma_4 > 46.06$ kg m^{-3}). This upper limit corresponds roughly to the upper temperature limit of AABW. The 2007 data are increasingly colder and fresher than the 1994/95 data on increasingly dense isopycnals for $\theta < 0°C$ in the trough and the basin. The envelopes of one standard deviation about the mean curves from the two realizations of the sections overlie each other through much of the water column, but diverge in the coldest, densest waters. These standard deviations are estimated from spatial variations of salinity along isopycnals within either each trough or basin. The temperature standard deviations on isopycnals are small enough in this region to neglect in this presentation. The 1994/5 standard deviations in the Princess Elizabeth Trough are noticeably higher then any of the others, perhaps owing to the reduced accuracies of the SR03 data mentioned earlier. However, even in the trough the θ–S envelopes are clearly distinct for $\theta < -0.2°C$.

While the near-bottom portions of the θ–S curves in the trough and the basin are colder and fresher on potential isopycnals in 2007 than in 1994/95, the bottom values themselves are fresher, lighter, and warmer in the later time compared to the earlier (Fig. 2). These bottom differences are consistent with the analysis of changes on isobars in the next section that reveal near-bottom warming, freshening, and decreasing density between 1994/95 and 2007. The abyssal waters in this region can warm and freshen on isobars even as they
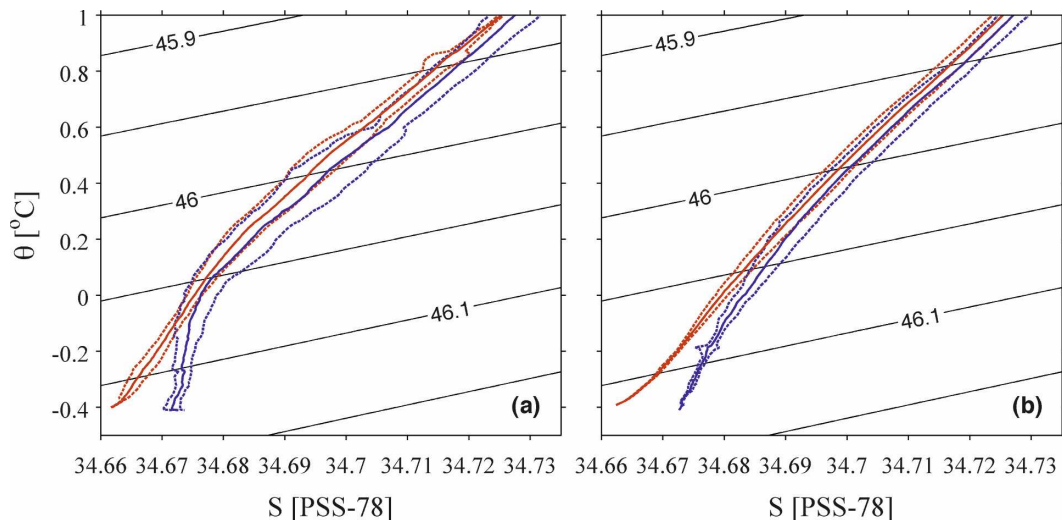
FIG. 2. Potential temperature–salinity (θ–S) diagrams for (a) the Princess Elizabeth Trough and (b) the Australian–Antarctic Basin from 1994/95 (blue) and 2007 (red). Means are solid and one standard deviation envelopes of salinity about the mean are dotted. Potential density relative to 4000 dbar (σ_4) is contoured at 0.05 kg m^{-3} intervals (black).

cool and freshen on isopycnals because pressures of abyssal isopycnal surfaces increase between 1994/95 and 2007, with some of the densest isopycnals found in 1994/95 disappearing altogether in 2007.

The 2007 mean θ–S curves are also slightly fresher ($\Delta S < 0.002$) than the 1994/95 curves for $\theta > 0.0°C$ in the trough and the basin. This difference is especially noticeable and uniform with temperature in the Australian–Antarctic Basin where the curves are quieter. This shift may simply be owing to remaining salinity standardization biases. The South Australian Basin mean θ–S curves (not shown) displayed a very similar shift through the deep ocean. In contrast, the 2007 Wharton Basin mean curve (not shown) is slightly and uniformly saltier than the 1994 curve. These offsets are all <0.002 in magnitude, near the expected measurement accuracies. Thus, adjustments beyond those already made for the standard seawater batch offsets are not warranted. The cruises for both realizations were interrupted by port calls between the South Australian and Wharton Basins that included changes of scientists and interruptions in sampling. These factors might contribute to these small apparent salinity biases among these basins.

In addition to these changes, the densest waters in the Australian–Antarctic Basin appear to have an AOU of about 2 μmol kg^{-1} lower in 2007 than in 1994/95 (Fig. 3). This difference is very small, but appears to increase with increasing density, like the change in the mean θ–S curve in this basin. Unfortunately, 1994/95 O$_2$ data from SR03 in the Princess Elizabeth Trough appear too noisy to make any inferences about the changes

in AOU there. No significant difference is apparent in the abyssal silicic acid concentrations in either basin. There was no noticeable change on abyssal isopycnals in basins to the north for either of these properties.

4. Isobaric water property variations

Means (θ) and differences ($\Delta\theta$) of abyssal potential temperature are estimated (Fig. 4). Differences are calculated by subtracting the 1994/95 data gridded on iso-
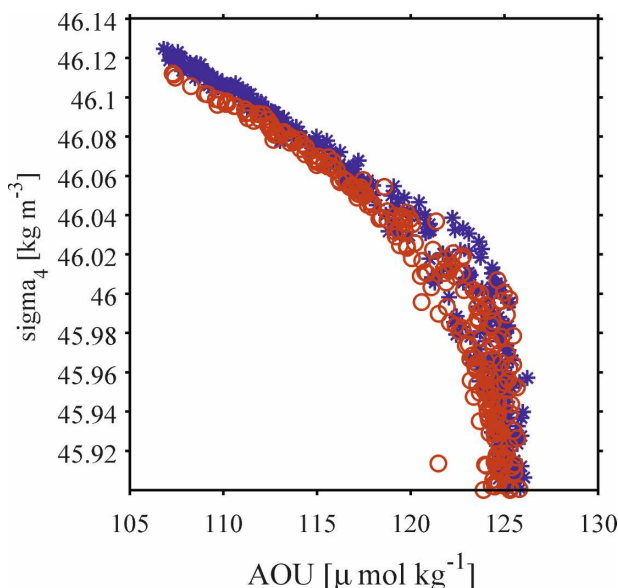
FIG. 3. AOU values from bottle data plotted vs σ_4 in the Australian–Antarctic Basin in 1994/95 (blue asterisks) and 2007 (red open circles).
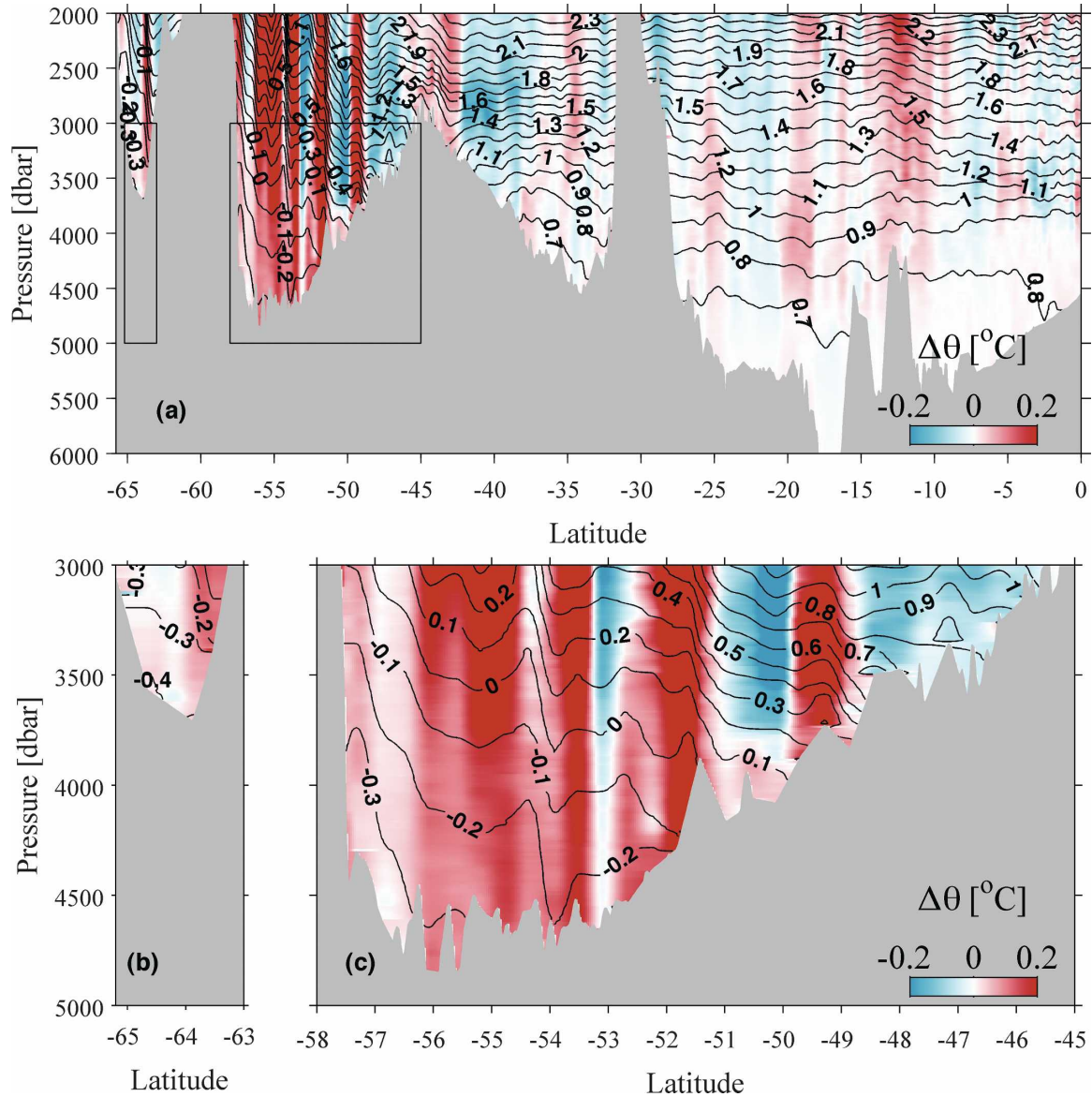
FIG. 4. Mean potential temperature θ (°C) isotherms (black, contoured at 0.1°C intervals) and differences $\Delta\theta$ (°C; colors) resulting from subtracting the 1994/95 from the 2007 data (gridded on isobars) along I08S/I09N. Red areas indicate warming and blue areas cooling with color saturation at ±0.2°C. (a) The section south of the equator from 2000 to 5000 dbar, (b) the Princess Elizabeth Trough from 3000 to 5000 dbar, and (c) the Australian–Antarctic Basin from 3000 to 6000 dbar are shown. The bottom bathymetry is shaded gray. The locations of (b) and (c) are outlined by black rectangles in (a).

baths from the identically gridded 2007 data. Vertically banded structures in $\Delta\theta$ are visible over the whole line (Fig. 4a). Such patterns might be anticipated in the ocean for vertical excursions associated with eddies, internal waves and tides, or meridional shifts in currents and fronts.

Mean potential temperatures generally trend colder toward the bottom and toward the south. The obvious upward trend of isotherms to the south throughout the water column, south of about 50°S, is typical of the Southern Ocean, with its deep-reaching, surface-intensified eastward-flowing Antarctic Circumpolar Current and its boundary currents of AABW, with westward flow increasing toward the bottom (e.g., Donohue et al. 1999). Vertical temperature gradients in the bottom several hundred decibars of each deep basin are generally reduced compared with the waters above. This pattern can be seen in the increasing vertical distances between isotherms approaching the bottoms of deep basins (Fig. 4).
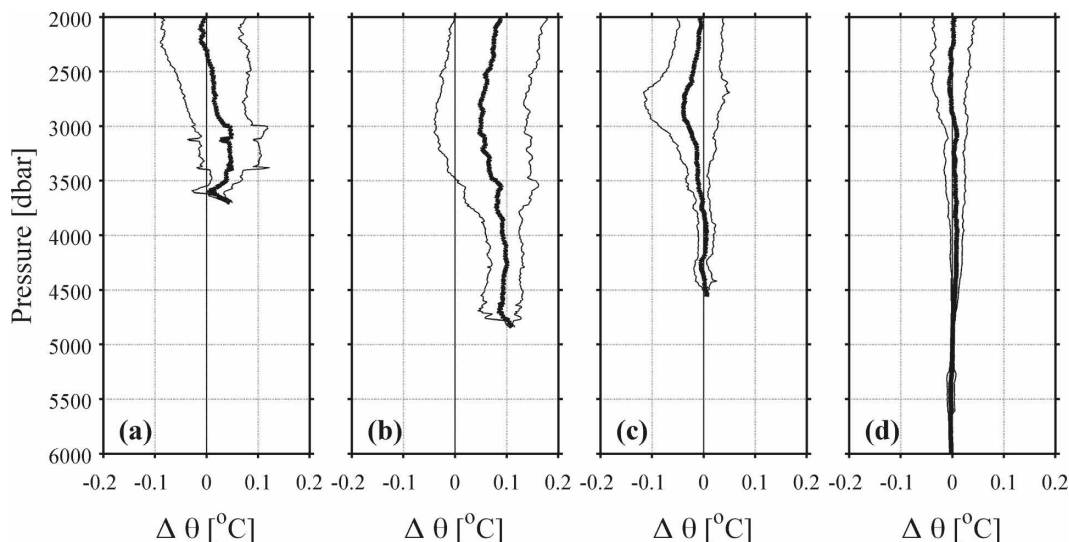
FIG. 5. Mean differences of potential temperature $\Delta\theta$ (°C) between 2007 and 1994/95 (thick black lines) below 2000 dbar with 95% confidence limits (thin black lines) for (a) the Princess Elizabeth Trough, (b) the Australian–Antarctic Basin, (c) the South Australian Basin, and (d) the Wharton Basin.

Basin-scale changes in potential temperature are most obvious below 3000 dbar in the two southern deep basins (Figs. 4b,c) and are not apparent anywhere below 2000 dbar in any of the basins to the north (Fig. 4a). The Princess Elizabeth Trough differences (Fig. 4b) show more warming north of 64°S than south of that latitude. This location is the dividing line between the 1994 SR03 data and the 1995 I08S data. Time variations taking place over the nearly 1-yr interval between these two sections may contribute to this pattern in the 2007 versus 1994/95 realizations. Also, the trough is not very wide, so eddies may strongly influence the result there. Warming predominates for $\theta < 0.1$°C ($P > 3000$–4000 dbar) in the wider Australian–Antarctic Basin (Fig. 4c). The coldest, densest, most recently ventilated AABW in both locations exhibits warming between 1994/95 and 2007.

Similar calculations and plots for changes in salinity (ΔS, not shown) revealed abyssal freshening of around 0.005 from 1994/95 to 2007 throughout the Princess Elizabeth Trough and the Australian–Antarctic Basin. This freshening was found for $\theta < 0.0$°C ($P > 2000$–3000 dbar) in the Australian–Antarctic Basin. Vertically banded structures showing increases and decreases in deep salinity were present to the north. However, as for $\Delta\theta$ in those regions, no basin-scale changes were obvious.

Ascertaining the statistical significance of $\Delta\theta$, ΔS, and dynamic height difference fields requires estimates of the effective number of degrees of freedom for these quantities. Integral spatial scales for each quantity studied at each pressure level in each basin are estimated

from integrals of autocovariances (e.g., Von Storch and Zwiers 1999) in latitude. The effective numbers of degrees of freedom are then computed by dividing the latitude ranges sampled at each pressure level and in each basin by the appropriate integral spatial scales. These effective degrees of freedom are used throughout the error analysis, including application of Student's t test for 95% confidence limits.

The mean $\Delta\theta$ at each pressure in the trough and three deep basins displayed with 95% confidence limits (Fig. 5) shows evidence of bottom water warming between 1994/95 and 2007 in the southern trough and basin and no significant change in the two northern basins. Warming in the Princess Elizabeth Trough reaches nearly 0.05°C for $3500 > P > 3000$ dbar, but is only different from zero at 95% confidence near 3500 dbar. Again, the trough is fairly narrow, so there are very few effective degrees of freedom there. However, in the wider Australian–Antarctic Basin warming reaches 0.1°C for $P > 3500$ dbar, where it is also easily different from zero at 95% confidence. The weak vertical stratification reduces the effects of mesoscale noise and the larger latitude range allows more degrees of freedom in this basin, compared with the trough to the south. In contrast, the two basins to the north of the Southeast Indian Ridge show no evidence of mean changes that are different from zero at 95% confidence anywhere below 2000 dbar.

Similar basinwide estimates of ΔS means and confidence limits (Fig. 6) indicate freshening in the southern basins. In the Princess Elizabeth Trough, freshening different from zero at 95% confidence is found nearly
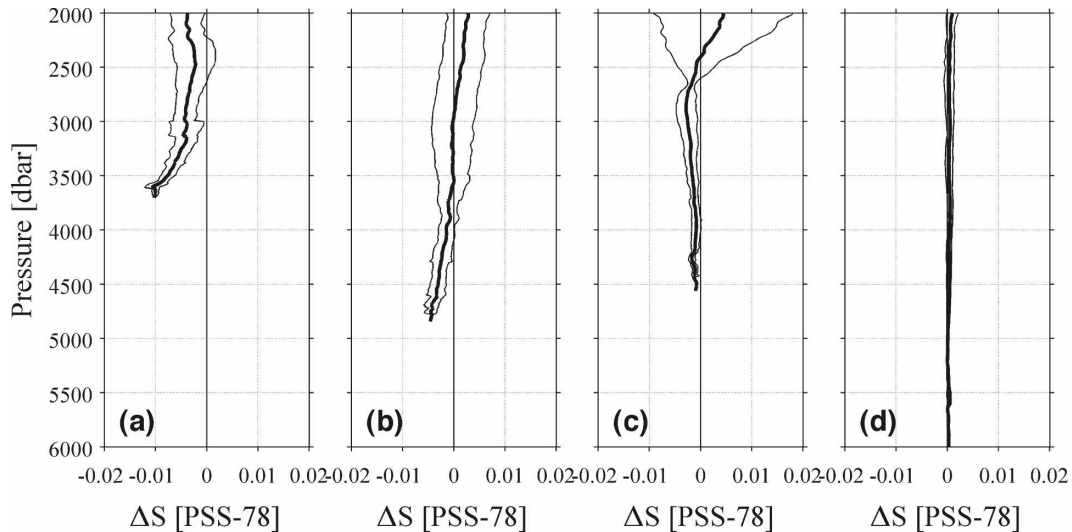
FIG. 6. Mean differences of salinity, S (PSS-78) below 2000 dbar between 2007 and 1994/95 (thick black lines) with 95% confidence limits (thin black lines) for (a) the Princess Elizabeth Trough, (b) the Australian–Antarctic Basin, (c) the South Australian Basin, and (d) the Wharton Basin.

everywhere below 2000 dbar, reaching 0.01 PSS-78 at the bottom around 3600 dbar. However, the accuracies of the SR03 salinities (0.005) in the Princess Elizabeth Trough should be borne in mind. In the Australian–Antarctic Basin, freshening different from zero at 95% confidence is found for $P > 4000$ dbar, and approaches 0.005 at the bottom, around 4800 dbar. In the South Australian Basin, a very slight freshening is suggested. While this freshening is statistically significantly different from zero at 95% confidence, at 0.002 it is within the possible range of the cruise-to-cruise standardization biases in salinity. There is no change of salinity evident in the Wharton Basin.

Abyssal warming and freshening both work to reduce density, so it is of interest to examine basin average changes in dynamic height (Fig. 7) to see how much these changes might contribute locally to steric sea level rise. Here the dynamic height calculations are made relative to 3000 dbar. In this case, the 3000-dbar "reference level" is not chosen in the spirit of the traditional level of no motion, but because it is generally below this level that statistically significant changes in both θ and S are found in both southern basins. In the Princess Elizabeth Trough, the mean dynamic height changes reach about 1 cm by the bottom relative to 3000 dbar. The difference in dynamic height values (Fig. 7) between the bottom and 2000 dbar demonstrates that warming and freshening between 2000 and 3000 dbar add another 1 cm to sea level rise. The dynamic height changes in the Australian–Antarctic Basin are more bottom intensified, with almost 4 cm of rise between 3000 dbar and the bottom, but only another

1 cm of rise between 2000 and 3000 dbar. In both southern basins the deep dynamic height changes are different from zero at 95% confidence. In the South Australian and Wharton Basins to the north, there are no significant changes in deep steric height. The deep warming and deep freshening found in the Princess Elizabeth Trough and the Australian–Antarctic Basin both contribute to the sea level rise.

5. Heat and freshwater fluxes

It would be interesting to know the magnitude of heat and freshwater fluxes in the formation regions of the abyssal waters that might be related to the warming and freshening patterns observed here. However, those estimates would be difficult to make because the sizes of the source regions are not known, the variations in abyssal water formation rates are not known, and the abyssal waters observed along the sections result from a complicated mix of source waters and physical processes.

Here a simpler means of putting the changes into context is used. Estimates are made of the average heat and freshwater fluxes that would be required to effect the temperature and salinity changes observed for $P > 3000$ dbar in the two southern basins if these fluxes were applied constantly over the time between repeats and over the lengths of the section deeper than 3000 dbar in each basin. The average heat flux that would be required to account for the changes in each basin is calculated using
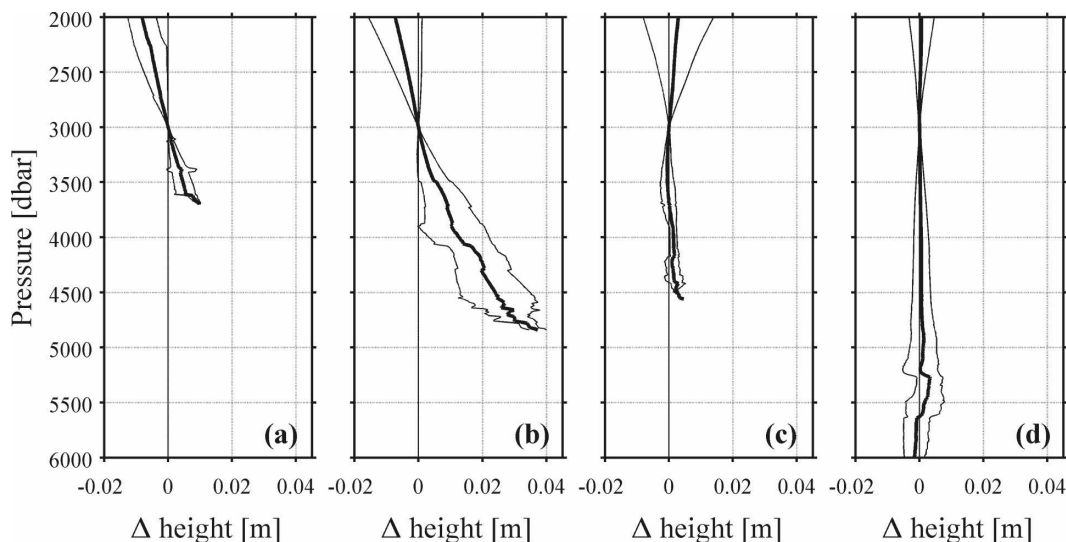
FIG. 7. Mean changes in dynamic water height (dynamic m) relative to 3000 dbar (thick black lines) shown below 2000 dbar between 1994/95 and 2007 with 95% confidence limits (thin black lines) for (a) the Princess Elizabeth Trough, (b) the Australian–Antarctic Basin, (c) the South Australian Basin, and (d) the Wharton Basin.

$$Q = \int_{3000}^{\text{bottom}} \frac{L(P)}{L(3000)} \left\langle \rho c_p \frac{T_f(P,y) - T_i(P,y)}{t_f(P,y) - t_i(P,y)} \right\rangle_y dP,$$

$$\text{(1)}$$

where Q is the heat flux, $L(P)$ the section length within the basin at every pressure, $L(3000)$ the length of the basin at the 3000 dbar level, ρ the time-mean in situ density, c_p the specific heat capacity, T the temperature, and t the time. Latitude is indicated by y, and a latitudinal section average over the portion of each basin sampled by $\langle \rangle_y$. Subscripts i and f represent initial and final times. A continuous heat flux of 0.2 W m^{-2} would have to be applied to the length of the section spanning the 3000-dbar level to effect the changes below 3000 dbar in the Princess Elizabeth Trough. By a similar estimate, a heating rate of 0.9 W m^{-2} would be required over the length of the Australian–Antarctic Basin spanning the 3000-dbar level to effect the changes observed below 3000 dbar there.

Similar calculations are made to quantify the freshening. For this quantity the average freshwater flux needed to achieve the freshening observed is calculated using

$$F = \frac{1}{S_o} \int_{3000}^{\text{bottom}} \frac{L(P)}{L(3000)} \left\langle \frac{S_f(P,y) - S_i(P,y)}{t_f(P,y) - t_i(P,y)} \right\rangle_y dP, \quad \text{(2)}$$

where F is the freshwater flux and S the salinity. Freshwater would have to be added at a rate of 2.5 mm yr^{-1} to the length of the section spanning the 3000-dbar level to effect the changes below 3000 dbar in the Princess

Elizabeth Trough. The same rate of freshwater deposition would be required over the portion of the Australian–Antarctic Basin spanning the 3000-dbar level to effect the changes observed below 3000 dbar there.

6. Transient tracer distribution

The concentrations of several chlorofluorocarbons (CFCs) in the atmosphere have increased rapidly during the past five decades and these increases can be modeled as functions of location and time (Walker et al. 2000). CFCs dissolve in surface seawater and are carried into the ocean interior by mixing and circulation processes. These compounds can be used as time-dependent, or transient, tracers, providing one method of assessing the relative time since a parcel of water has been ventilated by exposure to the atmosphere at the ocean surface.

Dissolved CFC-12 concentrations measured along the I08S/I09N section in 2007 (Fig. 8) reveal this ventilation process. In the Princess Elizabeth Trough, the Australian–Antarctic Basin, and to a lesser extent the South Australian Basin, CFC-12 concentrations in the abyssal waters indicate the presence of increasingly recently ventilated waters toward their bottom and southern boundaries.

A simple estimate of the apparent age (Doney and Bullister 1992) of a water sample CFC-12 measurement can be obtained by converting the measured concentration to a partial pressure, and then comparing this partial pressure to the atmospheric CFC-12 concentration
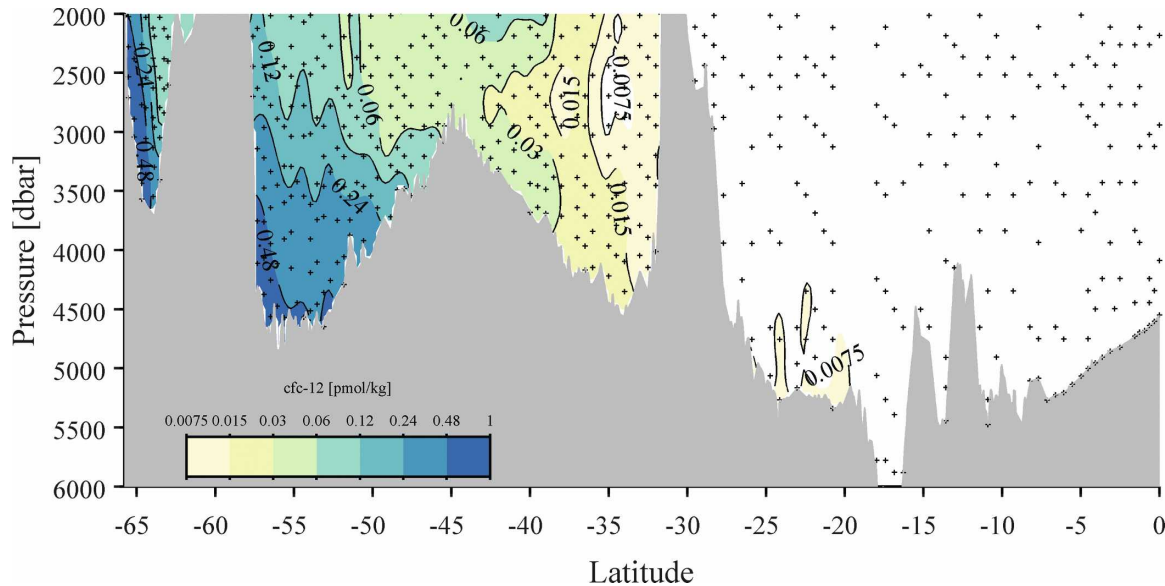
FIG. 8. Concentrations of CFC-12 measured along I08S/I09N in 2007 for the portion of the section south of the equator from 2000 to 6000 dbar contoured at doubling intervals from 0.0075 to 0.48 pmol kg^{-1}. Data (plus signs denote locations) were objectively mapped assuming a Gaussian covariance function with correlation length scales of 1° latitude and 500 dbar and a 0.1 noise-to-signal energy ratio. (Color palette by Cynthia A. Brewer, The Pennsylvania State University; available online at http://www.colorbrewer.org.)

history. Under some circumstances, these simple age estimates can be significantly biased from "ideal" ventilation ages (Thiele and Sarmiento 1990) because of the nonlinear atmospheric concentration histories of the CFCs, the finite time required for equilibration of these tracers at the surface, and the impacts of subsurface mixing. With mixing, instead of a single water mass age, there can be a distribution of transit times (Waugh et al. 2003) representing the different ventilation times of the individual components contributing to the water mass. The biasing effects on apparent ages resulting from mixing can be especially large in regions where a recently ventilated component undergoes strong mixing with surrounding waters with low tracer content, such as likely occurs along the pathways of AABW in this region of the southeast Indian Ocean. Nevertheless, in this case the CFC-12 apparent ages do provide a qualitative estimate of the time scales for the more strongly ventilated components of the water masses.

Concentrations of CFC-12 increase toward the bottom, showing that the coldest bottom waters in the Princess Elizabeth Trough and in the Australian–Antarctic Basin are the most recently ventilated (Fig. 8). In the bottom waters of these basins the CFC isopleths lie almost parallel to potential isotherms (Fig. 4). The most elevated concentrations of CFC-12 present in the abyssal waters in the Princess Elizabeth Trough and in the Australian–Antarctic Basin (<0.48 pmol kg^{-1}) correspond to apparent water mass age (not shown) of

about 40 yr. The distribution of transit times for the constituents of this water mass likely includes a substantial fraction that is younger than the apparent age, reflecting processes bringing recently ventilated surface waters to this region on time scales of a few decades or less, and a fraction that is significantly older than this age. Bottom CFC-12 concentrations measured along this section in the South Australian Basin are about an order of magnitude lower (<0.06 pmol kg^{-1}) than in the basins to the south, suggesting a substantial reduction of recently ventilated AABW north of the Southeast Indian Ridge. Even farther to the north in the Wharton Basin, the low but nonzero concentrations of CFC-12 (<0.015 pmol kg^{-1}, about 1% of modern surface equilibrium concentration values) found at the bottom from 25° to 20°S indicate that only a very small fraction of these abyssal waters has had contact with the atmosphere over approximately the past 55 yr.

These maxima in CFC-12 concentrations (and corresponding minima in the apparent ages) near the bottom and southern boundaries of the two southernmost basins (Fig. 8) are broadly reminiscent of the warming and freshening patterns observed there (Figs. 4–6) and provide a sensitive indicator of the pathways where perturbations in surface conditions can propagate into the interior of the ocean on decadal times. In contrast, the concentrations of CFC-12 in the abyssal waters of the Wharton Basin sampled by this section are close to the detection limit for CFC-12, and these waters show no

significant changes in temperature or salinity between 1994/95 and 2007.

7. Discussion

Repeat hydrographic data like those analyzed here provide one of the only datasets for assessing global changes in abyssal water properties. The cooling and freshening on abyssal isopycnals in the Princess Elizabeth Trough and Australian–Antarctic Basins analyzed here using repeat hydrographic section data are in accord with previous results in the region that were summarized in the introduction (Whitworth 2002; Jacobs 2004; Aoki et al. 2005; Rintoul 2007). While these previous results generally suggested cooling and freshening in the abyssal θ–S relation, they are somewhat more mixed as to changes in bottom temperature. Near the coast from 140° to 150°E the bottom waters appear to have cooled from 1950 to 2001 (Jacobs 2004). However, bottom warming is generally suggested in comparing 1936–93 data to 1994–96 data in the Australian–Antarctic Basin (Whitworth 2002), and an analysis of data taken from 65° to 60°S along 140°E in 1969–71, 1994–96, and 2002–03 does not suggest a monotonic trend in bottom temperatures (Aoki et al. 2005). Finally, while bottom temperatures were colder in 2005 than in 1995 off of the Antarctic Continental Rise at 115°E, they generally warmed over the last three decades or so in other locations around the Australian–Antarctic Basin based on analysis of 1970/71, 1994/95, and 2005 data (Rintoul 2007).

The addition of an isobaric analysis to an update along the lines of the previously published analyses of θ–S relations allows the quantification of heat and freshwater additions from 1994/95 to 2007 in the trough and three deep basins along the I08S/I09N sections, including their statistical significance, and their contribution to steric height changes. A contribution of 1 and 4 cm to steric height increases below 3000 dbar in the Princess Elizabeth Trough and Australian–Antarctic Basin, respectively, over the 12-yr interval is comparable in magnitude to a global average sea level rise of 3.1 ($\pm$0.4) mm yr^{-1} since 1993 (Nerem et al. 2006). However, there is considerable regional and temporal variability in sea level variations, and both ocean temperature changes and ocean mass changes contribute to the total.

The temperature changes below 3000 dbar in the Princess Elizabeth Trough and the Australian–Antarctic Basin amount to 0.2 and 0.9 W m^{-2}, respectively, when expressed as heat fluxes along the portions of the sections that extend to 3000 dbar or deeper. These fluxes are larger-than-average values of ocean floor heat flux data for 4500–3500 m that are roughly

0.05–0.1 W m^{-2} (Stein and Stein 1992). Hence, geothermal heat flux is unlikely to be the sole cause of observed changes. The salinity changes below 3000 dbar would amount to 2.5 mm yr^{-1} freshwater fluxes similarly expressed in both of these basins. Of course, the widths of the shelves over which these bottom waters are formed are considerably less than the widths of these basins. Thus, the effective heat and freshwater fluxes over the shelves would be considerably larger if changes in the surface fluxes near the formation regions were involved in these changes. The exact causes of the abyssal temperature and salinity changes are not clear. However, the CFC-12 data do suggest that they occur only in regions that have been ventilated during the past 55 yr or less. It could be that the changes observed are the result of some combination of changes in surface fluxes, changes in the water mass formation rates, and changes in the ratios of the various water masses that combine to form the AABW in these basins.

The changes in heat content of these two southern basins are comparable to the current global energy imbalance of 0.85 $\pm$ 0.15 W m^{-2} (Hansen et al. 2005). However, these two basins cover only a small fraction of the area of the earth, and the eastern Indian Ocean north of 45°S shows no evidence of abyssal heat gain in the I08S/I09N repeat sections analyzed here. Interestingly, temperature changes of similar magnitude have been observed over the last decade or so in the Weddell Sea (Robertson et al. 2002; Fahrbach et al. 2004), in the western basins of the South Atlantic, from the Scotia Sea all the way to the equator (Andrié et al. 2003; Johnson and Doney 2006; Zenk and Morozov 2007), and, to a lesser extent, in all of the main basins of the entire Pacific all the way to the Aleutian Islands (Fukasawa et al. 2004; Kawano et al. 2006b; Johnson et al. 2007). Together these abyssal changes may contribute significantly to the global heat budget.

Unlike the other two oceans, abyssal warming in the eastern Indian Ocean appears to be localized to the south of the Southeast Indian Ridge. Perhaps significantly, the ridge creates a barrier to abyssal spreading of the coldest AABW, with bottom values of $\theta > 0.4$°C (Fig. 1) found to the north of the sill at the Australian–Antarctic discordance (near 50°S, 126°E), which has a depth of around 4000 m (Smith and Sandwell 1997). The localization is consistent with the fact that only very low concentrations of transient tracers are seen to the north of the ridge, suggesting that mixing and dilution (Fine et al. 2008) en route may reduce the magnitude of the tracer signal (and any corresponding warming) in the abyss. It may be that changes in the bottom water would have to reach farther up in the water

column to cross over the Southeast Indian Ridge into the South Australian and Wharton Basins. It will be interesting to see if repeat sections in the western basins of the Indian Ocean reveal abyssal changes, because those basins may be fed more from the Weddell Sea than the eastern basins, as suggested by bottom potential temperature distributions (Fig. 1) and analysis of other properties (Mantyla and Reid 1995). Weddell Sea Deep Water ($-0.6 < \theta < 0.0°C$) and Warm Deep Water ($0.0 < \theta < 1.0°C$) have warmed in the past few decades within the Weddell Sea (Robertson et al. 2002), albeit with a recent partial reversal of that trend (Fahrbach et al. 2004).

REFERENCES

Andrié, C., Y. Gouriou, B. Bourlès, J.-F. Ternon, E. S. Braga, P. Morin, and C. Oudot, 2003: Variability of AABW properties in the equatorial channel at 35°W. *Geophys. Res. Lett.,* **30,** 8007, doi:10.1029/2002GL015766.

Aoki, S., S. R. Rintoul, S. Ushio, S. Watanabe, and N. L. Bindoff, 2005: Freshening of the Adélie Land Bottom Water near 140°E. *Geophys. Res. Lett.,* **32,** L23601, doi:10.1029/2005GL024246.

Barnett, T. P., D. W. Pierce, K. M. AchutaRao, P. J. Gleckler, B. D. Santer, J. M. Gregory, and W. M. Washington, 2005: Penetration of human-induced warming into the world's oceans. *Science,* **309,** 284–287.

Benson, B. B., and D. Krauss Jr., 1984: The concentration and isotopic fractionation of oxygen dissolved in freshwater and seawater in equilibrium with the atmosphere. *Limnol. Oceanogr.,* **29,** 620–632.

Bindoff, N. L., M. A. Rosenbeer, and M. J. Warner, 2000: On the circulation and water masses over the Antarctic continental slope and rise between 80° and 150°E. *Deep-Sea Res. II,* **47,** 2299–2326.

Doney, S. C., and J. L. Bullister, 1992: A chlorofluorocarbon section in the eastern North Atlantic. *Deep-Sea Res. I,* **39,** 1857–1883.

Donohue, K. A., G. E. Hufford, and M. S. McCartney, 1999: Sources and transport of the deep western boundary current east of the Kerguelen Plateau. *Geophys. Res. Lett.,* **26,** 851–854.

Fahrbach, E., M. Hoppema, G. Rohardt, M. Schröder, and A. Wisotzki, 2004: Decadal-scale variations of water mass properties in the deep Weddell Sea. *Ocean Dyn.,* **54,** 77–91.

Fine, R. A., W. M. Smethie Jr., J. L. Bullister, M. Rhein, D.-H. Min, M. J. Warner, A. Poisson, and R. F. Weiss, 2008: Decadal ventilation and mixing of Indian Ocean waters. *Deep-Sea Res. I,* **55,** 20–37.

Fukasawa, M., H. Freeland, R. Perkin, T. Watanabe, H. Uchida, and A. Nishina, 2004: Bottom water warming in the North Pacific Ocean. *Nature,* **427,** 825–827.

Gent, P. R., F. O. Bryan, G. Danabosoglu, K. Lindsay, D. Tsumune, M. W. Hecht, and S. C. Doney, 2006: Ocean chlorofluorocarbon and heat uptake during the twentieth century in the CCSM3. *J. Climate,* **19,** 2366–2381.

Gordon, A. L., S. Ma, D. B. Olson, P. Hacker, A. Ffield, L. D. Talley, D. Wilson, and M. Baringer, 1997: Advection and diffusion of Indonesian throughflow water within the Indian Ocean South Equatorial Current. *Geophys. Res. Lett.,* **24,** 2573–2576.

Gouretski, V. V., and K. P. Koltermann, 2004: WOCE global hydrographic climatology. Berichte des Bundesamtes für Seeschifffahrt und Hydrographie Tech. Rep. 35, 52 pp.

Hansen, J., and Coauthors, 2005: Earth's energy imbalance: Confirmation and implications. *Science,* **308,** 1431–1435.

Heywood, K. J., M. D. Sparrow, J. Brown, and R. R. Dickson, 1999: Frontal structure and Antarctic bottom water flow through the Princess Elizabeth Trough, Antarctica. *Deep-Sea Res. I,* **26,** 1181–1200.

Jacobs, S. S., 2004: Bottom water production and its link with the thermohaline circulation. *Antarct. Sci.,* **16,** 427–437.

Johnson, G. C., and S. C. Doney, 2006: Recent western South Atlantic bottom water warming. *Geophys. Res. Lett.,* **33,** L14614, doi:10.1029/2006GL026769.

——, S. Mecking, B. M. Sloyan, and S. E. Wijffels, 2007: Recent bottom water warming in the Pacific Ocean. *J. Climate,* **20,** 5365–5375.

Kawano, T., M. Aoyama, T. Joyce, H. Uchida, Y. Takatsuki, and M. Fukasawa, 2006a: The latest batch-to-batch difference table of standard seawater and its application to the WOCE onetime sections. *J. Oceanogr.,* **62,** 777–792.

——, M. Fukasawa, S. Kouketsu, H. Uchida, T. Doi, I. Kaneko, M. Aoyama, and W. Schneider, 2006b: Bottom water warming along the pathway of lower circumpolar deep water in the Pacific Ocean. *Geophys. Res. Lett.,* **33,** L23613, doi:10.1029/2006GL027933.

Levitus, S., J. Antonov, and T. Boyer, 2005: Warming of the world ocean, 1955–2003. *Geophys. Res. Lett.,* **32,** L02604, doi:10.1029/2004GL021592.

Mantyla, A. W., and J. L. Reid, 1995: On the origins of deep and bottom waters of the Indian Ocean. *J. Geophys. Res.,* **100,** 2417–2439.

Nerem, S. R., E. Leuliette, and A. Cazenave, 2006: Present-day sea-level change: A review. *C. R. Geosci.,* **338,** 1077–1083.

Rintoul, S. R., 2007: Rapid freshening of Antarctic Bottom Water formed in the Indian and Pacific Oceans. *Geophys. Res. Lett.,* **34,** L06606, doi:10.1029/2006GL028550.

Robertson, R., M. Visbeck, A. L. Gordon, and E. Fahrbach, 2002: Long-term temperature trends in the deep waters of the Weddell Sea. *Deep-Sea Res. II,* **49,** 4791–4806.

Rosenberg, M., R. Eriksen, S. Bell, N. Bindoff, and S. Rintoul, 1995: Aurora Australis Marine Science Cruise AU9407— Oceanographic field measurements and analysis. Antarctic Cooperative Research Centre Research Rep. 6, 97 pp.

Smith, W. H. F., and D. T. Sandwell, 1997: Global sea floor to-pography from satellite altimetry and ship depth soundings. *Science,* **277,** 1957–1962.

Solomon, S., D. Qin, M. Manning, Z. Chen, M. Marquis, K. B. Avery, M. Tignor, and H. L. Miller, Eds., 2007: *Climate Change 2007: The Physical Science Basis.* Cambridge University Press, 996 pp.

Speer, K. G., and A. Forbes, 1994: A deep western boundary current in the South Indian basin. *Deep-Sea Res. I,* **41,** 1289–1303.

Stein, C., and S. Stein, 1992: A model for the global variation in oceanic depth and heat flow with lithospheric age. *Nature,* **359,** 123–129.

Thiele, G., and J. L. Sarmiento, 1990: Tracer dating and ocean ventilation. *J. Geophys. Res.,* **95,** 9377–9391.

Von Storch, H., and F. W. Zwiers, 1999: *Statistical Analysis in Climate Research.* Cambridge University Press, 484 pp.

Walker, S. J., R. F. Weiss, and P. K. Salameh, 2000: Reconstructed histories of the annual mean atmospheric mole fractions for the halocarbons CFC-11, CFC-12, CFC-113, and carbon tet-rachloride. *J. Geophys. Res.,* **105,** 14 285–14 296.

Waugh, D. W., T. M. Hall, and T. W. N. Haine, 2003: Relation-ships among tracer ages. *J. Geophys. Res.,* **108,** 3138, doi:10.1029/2002JC001325.

Whitworth, T., III, 2002: Two modes of bottom water in the Aus-tralian–Antarctic Basin. *Geophys. Res. Lett.,* **29,** 1073, doi:10.1029/2001GL014282.

Zenk, W., and E. Morozov, 2007: Decadal warming of the coldest Antarctic Bottom Water flow through the Vema Channel. *Geophys. Res. Lett.,* **34,** L14607, doi:10.1029/2007GL030340.